Post Print DOI: https://doi.org/10.1016/j.adhoc.2021.102699

A Cooperative Crowdsensing System based on Flying and Ground Vehicles to Control Respiratory Viral Disease Outbreaks

Yesin Sahraoui[a,*], Chaker Abdelaziz Kerrache[b], Marica Amadeo[c], Anna Maria Vegni[d], Ahmed Korichi[a], Jamel Nebhen[e], Muhammad Imran[f]

[a] *Kasdi Merbah University of Ouargla, Ouargla, Algeria*
[b] *Laboratoire d'Informatique et de Mathématiques, Université de Laghouat, Laghouat, Algeria*
[c] *University Mediterranea of Reggio Calabria, Calabria, Italy*
[d] *Department of Engineering, Roma Tre University, Italy*
[e] *Prince Sattam bin Abdulaziz University, College of Computer Engineering and Sciences, P.O. Box 151, Alkharj 11942, Saudi Arabia*
[f] *College of Applied Computer Science, King Saud University, Saudi Arabia*

Abstract

The massive increase in population density in cities has led to several urban problems, such as an increment of air pollution, traffic congestion, and a faster spread of infectious diseases. With the rapid innovation in the intelligent sensors technology, and its integration into smart vehicles and Unmanned Aerial Vehicles (UAVs), a novel sensing paradigm has been promoted, namely *vehicular crowdsensing*, which leverages on-board sensors to capture information from the surrounding environment. Collected data are then analysed to take proper countermeasures. In this paper, we present a smart coordination mechanism between UAVs and ground vehicles (GVs), which sense information like body temperature and breathing rate of people, in order to support a variety of monitoring applications, including discovering the presence of infectious diseases. In our framework, namely GUAVA, aerial and ground vehicles are equipped with GPS devices and thermal cameras to monitor specific geographic areas, detect humans' vital parameters and, at the same time, discover duplicate data by identifying matching faces in thermal video sequences with the GaussianFace algorithm. The sensing tasks in hard-to-reach places are assigned to UAVs, with the ability to power up wirelessly from the nearest GV and offload the collected monitoring images to it. Simulation results have assessed our proposed framework, showing good performance in terms of distinct Quality of Service (QoS) metrics.

Keywords: UAVs; Covid-19; Crowdsensing; Sensors; Internet of Things; Internet of Vehicles.

1. Introduction

In recent years, the Mobile CrowdSensing (MCS) paradigm has made great technological leaps [1], thanks to the massive diffusion of mobile devices, ranging from smartphones to vehicles, equipped with different sensors, including cameras, gyroscopes and Global Positioning System (GPS) receivers. The huge amount of collected –and sometimes locally processed– data can feed a variety of smart city applications in different domains, like environment monitoring, intelligent transportation and even healthcare. In particular, MCS can cover a key role in discovering infectious diseases, like Covid-19, and/or predicting their spread. Several smartphone-based crowdsensing solutions have been developed with the aim of preventing Covid-19 infections [2, 3]. Similar approaches to fight Covid-19 disease have employed wearable sensors [4, 5], as well as crowdsensing solutions based on sensor-equipped vehicles, as the one proposed in [6].

So far, vehicles have been considered among the major contributors to MCS systems because, unlike other mobile devices, they do not have strict energy, storage and processing constraints [7]. At the same time, however, vehicles' movements are restricted to roads topologies that limit their crowdsensing capability. This shortcoming can be overcome by Unmanned Aerial Vehicles (UAVs), which can leverage high mobility and minimal costs to collect data at large-scale, potentially everywhere [8].

Nowadays, in such a world-wide pandemic scenario, UAVs are being considered for combating the Covid-19 disease [9], by assuming such mobile devices augmented with thermal cameras, in order to control and monitor social distancing and to gather vital parameters from wearable sensors for further analysis and processing on remote cloud facilities. However, despite the great flexibility and the highly dynamic mobility patterns provided by UAVs, these latter are still confronted with their limited lifetime, since their working time is constrained by the on-board battery capacity.

To cope against this intrinsic limitation and to exploit the best capability of vehicular technology, in this paper we propose GUAVA *i.e.*, a ground vehicle (GV) assisted UAV crowdsensing framework, that performs sensing tasks and real-time data collection across large-scale areas to prevent the spread of infectious diseases. In the proposed GUAVA framework, GVs assist UAVs in the pervasive data collection process, while also providing a prompt recharging mechanism. More specifically, the contributions of this paper are summarized as follows:

- We propose **GUAVA** (**G**round vehicle assisted **UAV** crowdsensing fr**A**mework) aiming to monitor geographic areas and collect vital parameters of people

*Corresponding author
Email addresses: sahraoui.yesin@univ-ouargla.dz (Yesin Sahraoui), ch.kerrache@lagh-univ.dz (Chaker Abdelaziz Kerrache), marica.amadeo@unirc.it (Marica Amadeo), annamaria.vegni@uniroma3.it (Anna Maria Vegni), ahmed.korichi@gmail.com (Ahmed Korichi), j.nebhen@psau.edu.sa (Jamel Nebhen), cimran@ksu.edu.sa (Muhammad Imran)

in smart cities, and even in unpaved areas or regions that are hard to reach from vehicles (*e.g.*, muddy roads, narrow streets of old cities, parks and stadium, etc.). Thermal cameras are used to capture images of the monitored areas and also body temperature and breathing rate parameters of people, which may be crucial to discover the presence of infectious diseases like Covid-19;

- We leverage the facial recognition technology built into thermal cameras to detect matching people faces and avoid duplicate data in the crowdsensing process; moreover, to solve the power system constraint, we assume that GVs carry wireless power chargers to recharge UAVs;
- Through extensive simulations and comparisons against benchmark schemes, we evaluate the effectiveness of our proposal GUAVA for collecting data in real time and in a realistic setting.

The rest of this paper is organized as follows. In Section 2, we introduce recent related works dealing with crowdsensing solutions, with a major focus on vehicular and healthcare applications. Differently from the state-of-the-art, GUAVA aims to contrast pandemic diseases, like Covid-19, through the exploitation of both UAV swarms and GVs, equipped with thermal cameras in order to detect and monitor infected people. Section 3 presents the proposed GUAVA framework, and the different tasks addressed by GVs and UAVs. In Section 4 we conduct the assessment of GUAVA's effectiveness, expressed in terms of both network performance and face matching accuracy. Finally, open challenges and conclusion are summarized in Section 5.

2. Related Works

In this section, we review existing research on mobile crowdsensing based on vehicular networks and UAVs. A detailed comparison of existing solutions presented in the following subsections is reported in Table 1, where different approaches are classified in terms of adopted paradigm (*i.e.*, IoV/VANET/UAV), architecture (*i.e.*, centralized (C) and decentralized (D)), accuracy (*i.e.*, low, medium, and high), cost, timeliness, energy constraints, coverage (*i.e.*, scalable, limited, and full), security issues, trustworthiness and reward.

2.1. Vehicle-based crowdsensing

In recent years, many researches have been conducted on vehicular crowdsensing applications with different targets, such as the monitoring of traffic in smart cities and, more recently, the support of healthcare services [10]. In parallel, multiple works have considered solutions to cope against the main open issues of the crowdsensing paradigm, like the support of privacy and trustworthiness and the definition of incentive mechanisms for vehicles. Some notable solutions are reported in the following.

Vehicular traffic applications. Wang *et al.* introduce the vehicular crowdsensing paradigm in public transports, which are characterized by scheduled and predictable trajectories [11]. An optimization problem has been designed to select the crowd of participants in order to maximize the spatial–temporal coverage. The authors prove that the selection of participants is NP-hard in large cities, and they adopt a greedy efficient combination query algorithm to solve the problem in a near-optimal fashion.

Xu *et al.* in [12] design a trustworthy vehicular crowdsensing framework, named TPSense, that augments Road Side Units (RSUs) with fog computing capabilities. RSUs acts as fog computing nodes for processing and storing event-reports; they collect information from nearby vehicles and share it with a remote cloud server, whenever needed. TPSense offers to vehicles data trustworthiness and privacy support through the use of blind signature technology, which allows to replace the identities of vehicles with random pseudonyms. Finally, in [13] Shao *et al.* present a vehicular crowdsensing scheme that gathers traffic information by taking road topologies into account. In the conceived design, sensing vehicles offload the collected data to sponsor vehicles located at the roads junctions. These latter perform a local processing and identify the traffic condition in real time. Computed results are then sent to a central server, which offers a global and updated vision of the traffic on a map.

Healthcare applications. A comprehensive discussion about how vehicular networking can help in fighting pandemics (and in particular Covid-19 disease) has been recently reported in [14]. The authors identify public transports as a fundamental means for collecting identity and health information of the passengers and their travel history. On-board sensors are able to recognize individuals that have intentionally broken the quarantine or people with Covid-19 symptoms, and they can send notifications to government authorities to take proper actions. For instance, in case a person is found to be infected, home quarantine can be issued for the passengers of the same public transportation.

In a previous work [6], Sahraoui *et al.* propose a framework based on the Internet of Vehicles (IoV) paradigm to control Covid-19 disease outbreaks in real-time. In the envisioned design, vehicles are augmented with thermal cameras to sense the pedestrians' body temperature and their breathing rate. Collected data are sent to an edge server where they are processed and displayed in the form of a heat map, tracking the potentially affected areas. Simulation results show that the proposed design exhibits good Quality of Service (QoS) metrics, expressed in terms of packet delivery ratio, delay, and throughput. In the same context, to reduce the spread of Covid-19 disease, the authors in [15] present a monitoring framework that leverages IoV and a deep learning objects detection algorithm through Faster Region-based Convolutional Neural Networks (Faster-RCNN), to provide real-time notifications about physical distancing violations.

Compared to these existing works, in this paper we present a hybrid crowdsensing approach, based not only on UAV devices, but assisted by ground vehicles, in order to guarantee an extended service coverage. The proposed GUAVA framework considers a data collection process based on a coordination mechanism between vehicles and UAVs.

2.2. UAV-based crowdsensing

Over the last few years, different literature works have focused on crowdsensing using UAVs in smart cities and wild environments, for emergency scenarios and health applications, such as the monitoring of infected people. As a matter, recently, the role of UAVs for combating infectious epidemics has largely been increasing.

Monitoring in smart cities. In [16], Barka *et al.* propose a distributed design based on UAVs for real-time urban traffic monitoring, in coordination with GVs and RSUs in a trustworthy manner. To provide crowd-related data without introducing additional overhead, the proposal focuses on the collection of Cooperative Awareness Messages, which include the current position, speed and direction of the vehicles, as defined by the European Telecommunication Standard Institute (ETSI) to support vehicular safety applications.

The use of a swarm of UAVs in urban environments for continuous video surveillance is introduced in [17]. There, to overcome the energy issue, a car-mounted landing platform is used as mobile charging station that allows UAVs to be powered based on a smart charging scheduling mechanism. In addition, a task coordination method is implemented to properly place the UAVs, by trading-off between the video surveillance requirement, *i.e.*, the continuous tracking of mobile ground targets, and the operational safety requirement. Another UAV-based video surveillance solution is reported in [18], where the authors assume that UAVs are equipped with face recognition sensors, working according to the Local Binary Pattern Histogram (LBPH) algorithm. Two use cases are considered in the experimentation: in the first case, videos are processed locally by UAVs, while in the second case, the processing is offloaded to a Mobile Edge Computing (MEC) server. Not surprisingly, the results demonstrate that, compared to the local processing, the MEC-based offloading approach reduces the computation time of face recognition and promptly detects suspicious persons, while also saving the scarce energy resources of UAVs.

Monitoring in wild areas. UAVs are a crucial means to monitor wild and rough areas. In this context, Zhang and Li in [19] present a framework based on UAV for remote sensing in regions that are not covered by public broadband networks. By combining 5G and Long-Range (LoRa) technologies, the proposed approach is able to perform data collection at high speed. Conversely, the authors in [20] study the use of a single UAV to collect data from clustered wireless sensor networks (WSNs) to monitor animals in wide and harsh areas. Two distinct data collection methods are considered. In the first one, the UAV visits all the cluster heads that received the sensing information from their cluster members. In the second one, in order to limit the energy consumption at the UAV and reduce the flight time, the cluster heads send the sensing information to a sink node that aggregates it and makes it available to the UAV.

Finally, the authors in [21] design a framework for disaster management using cloud-assisted UAVs. During their flying time, UAVs are configured to record videos of the disaster area and to perform a light pre-processing to filter out unnecessary frames. Then, the essential information is sent to the cloud for post-processing.

Monitoring and prevention of epidemics. UAVs can provide different services in healthcare scenarios, ranging from the remote delivery of medications, sanitization, masses screening and patient monitoring to the pervasive data collection of information that can prevent the spreading of infectious epidemics [22, 23]. Nowadays, with the Covid-19 outbreak, UAVs have been used in several countries to monitor crowds and give instructions to people not in compliance with social distancing guidelines. Moreover, if equipped with a thermal camera, they have been used for screening individuals and monitoring people's temperature and heart rates [23].

The work in [9] is the first attempt to provide a comprehensive UAV-based networked system to fight infectious epidemics like Covid-19. The proposal assumes that the geographic area to be monitored is divided into zones, each one assisted by a single UAV with a thermal camera. Two main services are provided, namely (*i*) to check the social distancing and sending alerts in case of violations and (*ii*) to collect people vital parameters from wearable sensors. The proposal also focuses on the design of a smart mobility algorithm that improves the movements of the UAVs in their zone and avoids collisions. However, it does not address strategies to cope against the main constraint faced by UAVs, that is the limited battery life.

Leveraging on the above motivations and open issues, in this paper we propose a crowdsensing platform where UAVs are assisted by GVs offering nearby wireless charging services. Similarly to other approaches [23], UAVs and GVs are augmented with thermal cameras that capture the temperature and breathing rate of people. To properly detect human body temperature through thermal cameras in GUAVA, we can refer to several existing works, including the International Organization for Standardization (ISO) guidelines on how to deploy thermal camera systems with high accuracy [1], and recent studies, like the one in [24]. There, it has been shown that, although sunlight conditions can impact on the body temperature measurements, thermal cameras provide the possibility of setting emissivity and reflected temperature compensation to cope against this issue and provide reliable results. In addition, in order to avoid that data from the same person are wrongly collected multiple times, we leverage a high performing facial recognition algorithm to discard redundant data.

[1] See ISO/TR 13154:2017 at https://www.iso.org/standard/69347.html).

Table 1: Comparison of the existing schemes.

Existing scheme	Paradigm	Architecture	Accuracy	Cost	Timeliness	Energy constraints	Coverage	Security&Privacy	Trustworthiness	Reward
Sahraoui *et al.* [6]	IoV	D	high	low	high	low	scalable	✓	✓	✗
Sahraoui *et al.* [15]	IoV	D	high	low	high	low	scalable	✓	✓	✗
Xu *et al.* [12]	IoV	D	high	low	high	low	n/a	✓	✓	✗
Elbir *et al.* [14]	IoV	D	hight	low	low	low	limited	✗	✗	✗
Shao *et al.* [13]	VANET	C	low	low	medium	low	scalable	✗	✗	✗
Wang *et al.* [11]	VANET	C	medium	medium	high	low	scalable	✗	✗	✓
Yi *et al.* [25]	VANET	C	low	low	high	low	limited	✗	✗	✓
Barka *et al.* [16]	UAV/VANET	D	high	medium	high	high for UAV	limited	✓	✓	✗
Trotta *et al.* [17]	UAV/VANET	D	high	medium	high	low	scalable	n/a	n/a	✗
Motlagh *et al.* [18]	UAV	C	medium	low	high	medium	full	✗	✗	✗
Vera-Amaro *et al.* [20]	UAV	C	high	high	high	high	full	✗	n/a	✗
Zhang and Li [19]	single UAV	C	high	low	high	high	scalable	n/a	n/a	✗
Luo *et al.* [21]	UAV	C	high	low	high	high	full	✗	✗	✗
Our proposal	UAVs/IoV	D	high	low	low	low	full	✓	✓	✗

3. GUAVA Framework

This section describes the GUAVA framework and its main tasks. Specifically, we first introduce the reference system model, where UAVs and GVs collaborate for data sensing and transmission. The algorithm for the detection and alerting of infected people is then presented in Subsection 3.2, while the face recognition approach is described in Subsection 3.3.

3.1. System model

The gathering process can be performed during night and day and even in difficult circumstances, since thermal cameras work efficiently even in low light conditions, and they are generally not affected by adverse weather, including fog, rain and high temperatures. As shown in Figure 1, the proposed GUAVA crowdsensing system includes aerials and ground vehicles (in the following simply referred to as *collectors*), equipped with thermal cameras and GPS devices to collect (*i*) images of the monitored area and (*ii*) body parameters of the people present in the monitored area. Data are then sent to a Collection Center for further processing.

In the following, we provide a description of main entities and related tasks of GUAVA framework, with reference to Figure 1.

Collectors. GVs and UAVs are collector nodes that work cooperatively to perform the sensing tasks and ensure full coverage in the designated area. While GVs operate on some predefined streets, as determined by government and local authorities, UAVs are remotely controlled[2] to fly at low altitudes and collect data in rough areas, especially those that are difficult to access by GVs, such as stadiums, parks, etc.

The considered thermal cameras combine facial recognition and vital sign monitoring functions. They are configured to provide a surveillance service of the monitored area and to measure in real time with high precision two parameters of the people there present, namely (*i*) body temperature and (*ii*) breathing rate, which are widely used to assess the degree of infection of respiratory diseases like Covid-19 [26]. Specifically, to properly measure the breathing rate of people in places of mass gathering, we refer to the approaches designed in [27, 28]. It was shown that the breathing rate can be inferred from images captured by thermal cameras by monitoring how the temperature of the nasal area changes during inhalation and exhalation. As a result, the temperature of the nasal region increases during exhalation and decreases during inhalation and the thermal camera can capture such a variation. The respiration rate is then determined from the breath-to-breath intervals.

When the sensed body temperature exceeds the threshold of 38°C and the breathing rate is higher than 30 times/minute, the collectors detect a potential

[2] We assume that a remote Control Center is in charge of remotely monitoring the missions of UAVs.

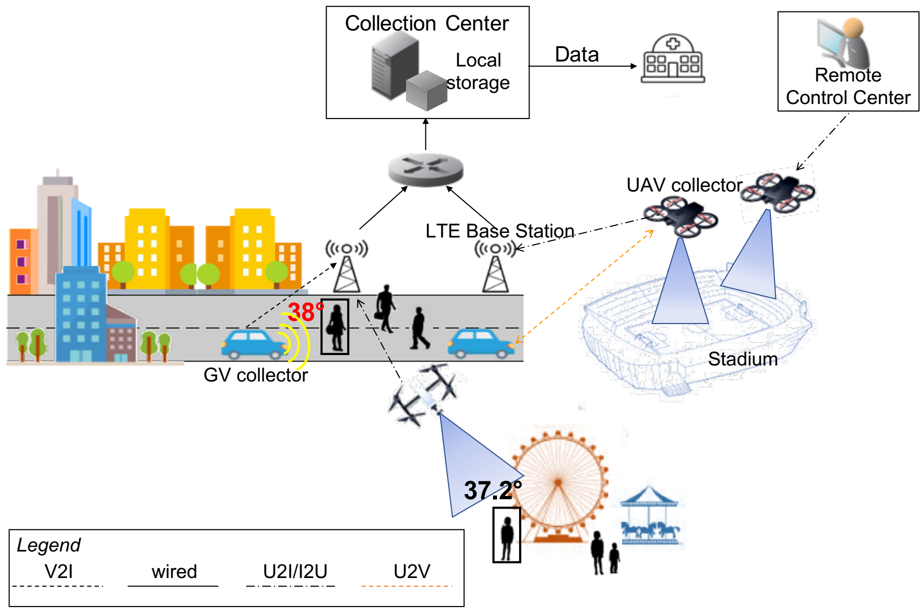

Figure 1: General design of our GUAVA framework.

infected individual. In addition, to avoid duplicate sensing data, a face recognition algorithm is implemented by the Collectors. Based on facial landmarks extraction, the method is able to detect matching faces with high accuracy [29], according to some features such as distance between the eyes, ears shape and size, nose size, lip shape, as it will be clarified in the next section.

When performing their mission in a certain geographic area, the collectors associate the sensed body parameters (*i.e.*, breathing rate and temperature) to the corresponding human face. Then, by accessing the previous collected information, they check if the same person has been already sensed. If a matching is found, then the information is discarded; otherwise, it is transmitted to an edge server, where the data Collection Center is located, as it will be clarified in the following. As a result, if the collectors encounter the same person multiple times during their mission, no redundant data is transmitted.

To cope against the power limitations of UAVs, which mainly depend on the distance traveled during hover time and the speed, we assume that every GV is equipped with a wireless power charger on its roof. When the battery level of a UAV drops below a certain threshold, a notification is sent to the Control Center, which promptly redirects it to the nearest power supply vehicle. Notice that several variables can impact on the UAV's power consumption, including aerodynamic layout and structure design of the device, the weather conditions, the service type, the battery type, the hour of the day and the use of solar power as energy resource [30]. Therefore, it is not possible to provide an *a priori* precise estimation of the duration of the UAV battery. However, recent works like [31, 32, 33] have shown that, on average, recent UAVs are able to flight with a sensor payload, *e.g.*, camera and GPS device, for about 30 minutes of time with a fully-charged battery. This allows the full coverage of many hard-to-reach areas. However, in the presence of large areas or when many people have to be sensed, multiple UAVs can be simultaneously used to avoid the interruption of the service and the consequent QoS degradation. In our proposal, each UAV is responsible for a specific area that is not overlapping with the other UAVs monitoring areas. As an instance, Figure 2 shows the case of four UAVs monitoring adjacent areas where UAVs mobility follows a growing helical rectangular trajectory. With an average speed of 20 m/s, a range of 200 m, and a rectangle enlargement of 200 m at each step, a single UAV can cover about 1 km^2 every half an hour, considering that according to the recent developments the average flight time of UAVs is about 30 minutes.

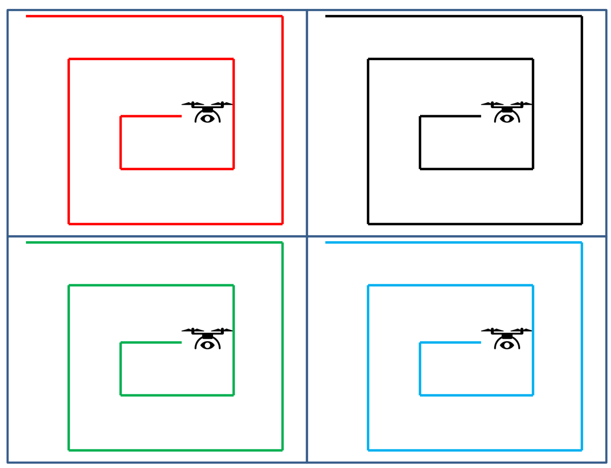

Figure 2: Example about UAVs monitoring trajectory.

Collection Center. Sensed data are sent to a *Collection Center*, which consists of an edge server offering local storage and additional low-delay data processing. While GVs transmit in real time both surveillance images and body parameters to the Collection Center, UAVs are programmed to stream only the body parameters, which are supposed to be smaller in size *i.e.*, a few kbytes. More specifically, each data unit includes the person's geolocation information, body temperature, and breathing rate. In addition, a flag is associated to every data unit showing if its source is a UAV or a GV. To save energy resources, UAVs offload the collected surveillance images to the GV during the re-charging process. This latter will then forward the images to the Collection Center.

The main target of Collection Center is to maintain a database of the monitored areas and to create a heatmap showing the geographical areas where there are potentially infected people. By visualizing the heatmap, government authorities can issue additional control checks in the potentially affected area to prevent the spread of the disease.

By following the 3GPP-V2X (vehicle-to-everything) specification in [34], the Collection Center can be implemented as a V2X Application Server according to the Multi-Access Edge Computing (MEC) paradigm. By providing storage and computing resources close to where data are produced, the Collection Center ensures that data are processed in real-time at the network edge thus also limiting the traffic load in the core network. Multiple Collection Centers can be deployed in different geographic areas and their storage and processing resources can be sized according to the estimation of the amount of data that are received. Depending on their role, the interested consumers can access the data from a Collection Center or from multiple ones. For instance, Health Department Inspectors working on a specific area will access only the data from that area; vice versa, if the Health Ministry is interested in an overall map of the suspected infection cases, the data from multiple Collection Centers will be accessed.

Communication. To ensure low delay in the data delivery process, the communication between Collectors and Collection Center leverages 4G/5G Long Term Evolution (LTE) connectivity. As depicted in Figure 1, aerial and ground vehicles transfer the sensed data to LTE base stations through, respectively, UAV-to-Infrastructure (U2I) and Vehicle-to-Infrastructure (V2I) communications. The base stations then forward the information to the edge server via wired links. Finally, UAV-to-Vehicle (U2V) connectivity is used during the recharging process to offload the surveillance images from the UAV to the GV.

Notice that, in GUAVA framework, in order to limit the energy consumption, we neglected to implement an additional communication exchange between UAVs for discarding possible duplicate data, *e.g.*, caused by people moving between areas covered by distinct devices. As for the redundancy caused by ground vehicles and UAVs monitoring the same area, we recall that collected data is labeled with time and GPS position before being sent to the Collection Center. This latter can then perform a spatio-temporal overlapping to filter out the redundant data. Also, for energy issues, the GUAVA framework is not able to track specific people who move between collectors, but it reports an estimation of the areas where possible infectious cases are present, in order to take proper countermeasures.

3.2. Remote sensing process

The pseudocode of the conceived GUAVA crowdsensing process is presented in Algorithm 1. Let us assume that the data collectors consist of a set of GVs, *i.e.* $G = \{g_1, g_2, \ldots, g_N\}$ with $N \in \mathbb{N}$, and a set of UAVs, *i.e.* $U = \{u_1, u_2, \ldots, u_M\}$ with $M \in \mathbb{N}$. Each collector is assigned to a geographic area in order to collect surveillance images and vital signs of the available people, represented as a set $P = \{p_1, p_2, \ldots, p_K\}$ with $K \in \mathbb{N}$. The localisation of the i-th GV (*i.e.*, g_i with $i \leq N$) can be captured by the local GPS device as $\overrightarrow{l}_{g_i} = (x_{g_i}, y_{g_i})$. Similarly, the localization of the j-th UAV (*i.e.*, u_j with $j \leq M$) can be expressed as $\overrightarrow{l}_{u_j} = (x_{u_j}, y_{u_j}, z_{u_j})$.

The k-th person ($i.e.$, p_k with $k \leq K$) is identified by its face, and has a 2D location information compared to GVs $i.e.$, $\overrightarrow{l}_{p_k} = (x_k, y_k)$, and a 3D location information compared to UAVs $i.e.$, $\overrightarrow{l}_{p_k} = (x_k, y_k, z_k)$. In order to be detected, the k-th person must be within the sensing range of the i-th GV $i.e.$, $r_s^{(i)}$, or within the sensing range of the j-th UAV $i.e.$, $r_s^{(j)}$, as follows:

$$\|\overrightarrow{l_{g_i}} - \overrightarrow{p_k}\| \pm \varepsilon \leq r_s^{(i)} \quad \text{OR} \quad \|\overrightarrow{l_{u_j}} - \overrightarrow{p_k}\| \pm \varepsilon \leq r_s^{(j)}. \tag{1}$$

where we included the absolute error ε defined as $\varepsilon = \|d_m - \tilde{d}\|$, with d_m [m] as the measured distance and $\tilde{d}$ [m] as the estimated one.

Based on the experimental results in [35, 36], Long-Wave Infrared (LWIR) thermal cameras on-board of UAVs and GVs are able to recognize human faces from a distance of 30 m with 100% accuracy, but reasonably the face recognition performance decreases as the distance increases. No sensing can be performed when the distance exceeds 90 m. Therefore, we set the maximum sensing range for adequately detecting people's parameters in our framework to the value of 30 m, $i.e.$, $r_s^{(i)} = r_s^{(j)} = 30$ m.

As defined in [37, 38], the following threshold values for, respectively, body temperature and breathing rate are used to detect a potentially infectious individual, namely $\tau_1 = 38$ °C, and $\tau_2 = 30 times/min$.

An individual p_k is considered potentially infected if, and only if, its sensed body temperature $\overrightarrow{V}_{s1,k}$ and the sensed breathing rate $\overrightarrow{V}_{s2,k}$ are higher than given thresholds τ_1 and τ_2, respectively, $i.e.$,

$$\overrightarrow{V}_{s1,k} \geq \tau_1 \ \text{ AND } \ \overrightarrow{V}_{s2,k} \geq \tau_2, \tag{2}$$

and we also considered the temperature measurement response time $\overrightarrow{T}_{s1}$ and the breathing rate measurement response time T_{s2} should be lower than given thresholds ($i.e.$, $val_{1,2}$ [ms]), such as:

$$\overrightarrow{T}_{s1} \leq val_1 \ \text{ AND } \ \overrightarrow{T}_{s2} \leq val_2. \tag{3}$$

Data from different collectors are integrated to support decisions at the Collection Center. Specifically, we assume to have a data table as a form of triplet $i.e.$, $< infected\ case,\ GPS\ coordinates,\ face\ image >$, associated to a given collector responsible to the data acquisition. Notice that redundant data are omitted in this work. If the sensed parameters are associated to a face that does not match any other previously detected, they will be considered as a new potential infectious case. Therefore, GVs send the sensed (and not redundant) vital signs satisfying the above mentioned condition expressed in Eq. (2), directly to the Collection Center, together with the images of the monitored area. Being represented with the tuple {*geo-localization*, *temperature*, *breathing rate*}, the collected parameters allow to identify the position of possibly infected people and to take additional countermeasures. Conversely, to save energy resources, UAVs transmit in real-time only the sensed parameters and temporarily cache the surveillance images. As shown in Algorithm 1, these latter will be offloaded during the re-charging process to the closest GV and then sent to the Collection Center. Notice that the sensing process of the j-th UAV occurs if its energy level (*i.e.*, $\mathcal{E}_{u_j}$) is enough to accomplish this task *i.e.*,

$$\mathcal{E}_{u_j} > \chi, \tag{4}$$

where χ is a given energy threshold. If Eq. (4) does not hold, the j-th UAV computes the distance to the closest GV *i.e.*,

$$\min_j d_{u_j,g_i}, \ \forall g_i \in G, \tag{5}$$

in order to move to that position (*i.e.*, $\overrightarrow{l_{g_i}}$) and recharge its battery level, as well as offload the set of collected images. Notice that the UAV can move autonomously to the nearest GV or also driven by the Control Center.

Finally, when the monitoring process in the designed area has been completed (*i.e.*, the whole area has been covered) the collectors can be assigned to a new one.

3.3. Face recognition process

Deep Neural Network. The face recognition process used in our GUAVA framework leverages existing studies on deep neural network architectures [39] and consists of the following steps *i.e.*, (*i*) localization of human face in the video images –*face detection*– using bounding boxes, (*ii*) normalization of the face to extract features from it and, finally, (*iii*) classification –*face recognition*–, in order to find the matching faces based on existing database. The deep neural network architecture for face recognition consists of a convolutional layer as a set of trainable filters, then the input passes through the pooling layer to reduce its spatial size [39]. The output of convolutional/pooling layers is flattened and fed it into a fully connected layer, to be classified using an activation function.

As expected, the use of this architecture has led to a massive increase in the performance, which has approached and, in recent times, even exceeded the human level capacity. Nevertheless, some conditions still affect the performance of face recognition, including head poses, illuminations, facial expressions and occlusions [40].

GaussianFace model. To improve the face recognition performance and avoid the transmission of duplicated sensing, in this paper we propose to use the GaussianFace model, originally described in [29], which is one of the best tools currently available to capture matching faces from images obtained by surveillance cameras. The GaussianFace model surpasses humans-level performance in identifying matching faces, reaching the accuracy ratio of 98.52%, as compared to 97.53% for humans, when using the Labeled Faces in the Wild (LFW) dataset [41].

As shown in Figure 3, after detecting the human face and extracting it from a streaming video, the facial feature extraction process begins with adjusting the thermal input image to a specific size *i.e.*, 150×120 pixels, depending on

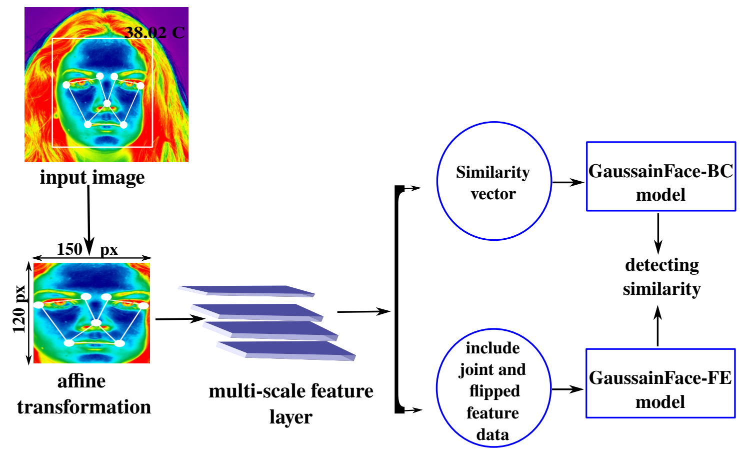

Figure 3: GaussianFace model for face verification used in GUAVA framework.

some facial landmarks, including both mouth corners, eyes and nose. Then, each face image is divided into overlapping regions of 25×25 pixels, the multi-scale uniform LBP histograms are extracted in each region, and create a feature vector. In the face recognition stage, this model is used either as a Binary Classifier (GaussianFace-BC) or as a Feature Extractor (GaussianFace-FE) and compares the face with a given face dataset to match similar faces and reveal similarities.

In our scenario, the GaussianFace model is selected to avoid duplicate crowdsensing data. Firstly, we measure the similarity vector $x_i = (x_1, x_2, \ldots, x_p)^T$ between a pair of face images A and B as an input to the GaussianFace-BC model, or the joint feature vector $x_i = [(x_i^A)^T, (x_i^B)^T]^T$ with its flipped version $x_i^{flipped} = [(x_i^B)^T, (x_i^A)^T]^T$, as an input to the GaussianFace-FE model. Then, we perform the assessment of the latent vector $\overrightarrow{F}$, in a similar way as in [42], as each input point x_i has a latent variable f_i. Then, we use a squashed function in order for the output y_i to be into $[0, 1]$, $\Pi(f_i) = p(y_i = 1|f_i)$. Finally, we predict the matching face image(s).

4. Experimentation

In this section, we evaluate the proposed GUAVA design by first targeting two main aspects *i.e.* (i) assessing the efficiency of the selected face recognition process and (ii) assessing the QoS of the overall crowdsensing process.

Then, we compare GUAVA against a benchmark crowdsensing platform, namely BUCST [16] in terms of (i) amount of monitored area over time, (ii) traffic overhead. Finally, we focus on the energy consumption issue and an optimization process related to the minimization of the number of GVs and UAVs, subject to performance requirements, is investigated.

4.1. Simulation setup and performance metrics

To assess the QoS of the proposed crowdsensing process, we leveraged the Network Simulator 3 (ns-3) software to build the reference scenario as in Figure 1, where a set of collectors perform the crowdsensing service in a city area and send the collected parameters to the edge server of the Collection Center. In particular, we considered a set of pedestrian users walking the streets of the Annaba city center (Algeria). There, GVs move according to the realistic Simulation of Urban MObility (SUMO) model [43], while UAVs move according to the Gauss Markov Mobility Model in 3D environment [44]. This mobility model assumes that when the UAV gets closer to an obstacle, it will change its direction to avoid collisions; it thus depicts a more realistic behavior for UAVs. Of course, we are aware that realistic flight conditions can strongly impact on the UAV mobility, as well as on the energy consumption and the QoS metrics, causing higher delay and lower throughput. However, UAV flight conditions can be corrected by the Control Center that can intervene in some cases, such as to redirect the UAV to the nearest GV for wireless charging.

To simulate the collection of vital signs from the pedestrian users, possibly affected by Covid-19, we considered the daily average number of Covid-19 cases reported by the local authorities in the area, during the past autumnal months, w.r.t. the population density. Based on this value, we created a synthetic data set, as in [45], that we imported in ns-3 to randomly simulate the presence of potential infectious people in the scenario. Table 2 summarizes the considered simulation settings.

To evaluate the performance of our GUAVA proposal in ns-3 environment, we used the following metrics:

- **Packet Delivery Ratio (PDR)**, which expresses the ratio of packets sent by the Collectors that have successfully reached the Collection Center. We assume that the sensed information per each potentially infectious individual, as described in Section 3, fits a single data packet;
- **End-to-End (E2E) delay** d_{e2e} [ms], which expresses the time interval since the packet has been transmitted from the source (*i.e.*, UAV or GV) to the instant when it reaches the Collection Center successfully;
- **Throughput** Θ [Kbit/s], which refers to the number of bits per second that are successfully delivered to the Collection Center;
- **Mean jitter or delay variation** [ms], which refers to the variation in the delay of packets delivered to the Collection Center.

For face matching evaluation, we used facial images obtained from FERET dataset [46] that were normalized to a size of 150×130 pixels in order to obtain equal footing and allow processing and features extraction. The training dataset for the recognition test consisted of 100 images, and we used a gallery as reference set consisting of 1000 images, and one probe set containing 623 images with different facial expressions, such as smile, astonishment, contempt, fear, and anger.

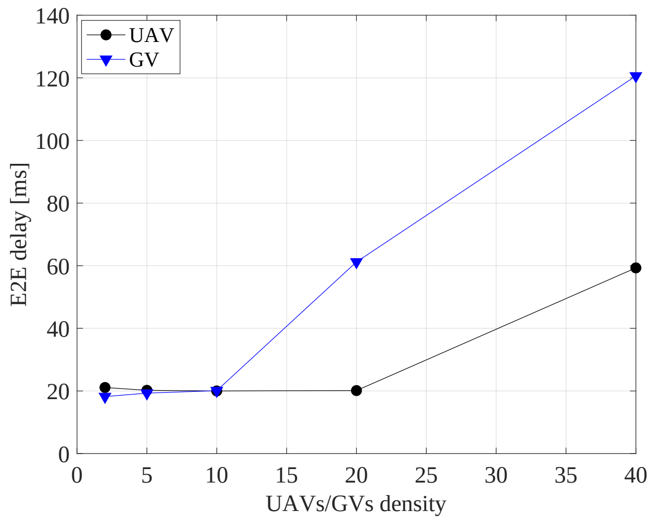

Figure 4: E2E (network) delay vs. the UAVs/GVs density.

To estimate the accuracy of the recognition process, we considered the recognition rate or success rate metric, which is calculated by dividing the correctly identified probe images on the total testing samples.

4.2. Results

In this subsection, we first assess the accuracy of the selected GaussianFace-FE recognition process and then we investigate the performance of the GUAVA proposal in terms of the above mentioned QoS metrics.

4.2.1. Accuracy of the face recognition algorithm

As shown in Table 3, we consider the selected dataset and compare it against gallery images. The dataset contains images of facial expressions and provides a high success rate (and a consequent low error rate, i.e, only 3.69%) with low training. The model is typically highly accurate, but it can be affected by the A-PIE (Ageing, Pose, Illumination, Expression) problems for face recognition.

It can be generally observed that the GaussianFace algorithm is a very efficient approach in term of accuracy at the expenses of a slightly high delay, *i.e.*, about 1.02 s per face recognition with i-5 4300U CPU @1.90 GHz processor speed and 4 GB RAM, without dedicated graphic card. In particular, when considering the overall E2E delay per each crowdsensed information, which includes the time needed for data sensing, face recognition and data delivery to the Collection Center, we can notice that the major contribution is due to the face recognition.

To better assess this aspect, we distinguish the network delay (needed for the data delivery) and the recognition delay. Figure 4 illustrates the network

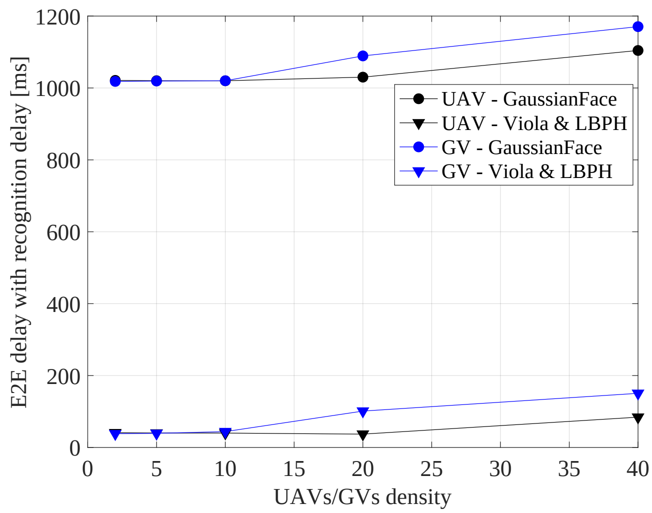

Figure 5: Total E2E delay vs. the UAVs/GVs density.

delay *i.e.*, d_{e2e} [ms], when varying the UAVs/GVs density (without taking into account the delay introduced by the face recognition process). It shows that the use of LTE technology in UAVs and GVs provides an extremely low E2E delay, which does not go beyond 120 ms. As the density of the collectors increases, the delay increases due to the higher chances of packet collisions. Vice versa, Figure 5 shows the total E2E delay, which is higher due to the impact of the face recognition process. The targeted monitoring application can however tolerate such a delay, which is lower than 1.2 s even in the worst case.

It is worth observing that there are multiple available face recognition algorithms in the literature, some of them are faster than the considered GaussianFace algorithm but also less accurate. For instance, when we tested a traditional algorithm for face detection, *i.e.*, the Viola Jones' algorithm [47], which uses the Haar Classifier for face detection, and couples it with a real-time face recognition pattern, using the LBPH algorithm, the average time taken per frame for face recognition is about 34.90 ms. The price to pay is however the lower accuracy, *i.e.*, a higher false positive rate. In our scenario, this also means that the system would not be able to properly recognize duplicate sensed information, which is instead crucial in our design. Therefore, we recommend selecting a successful recognition algorithm like GaussianFace.

Finally, to study the feasibility of adding other features besides the facial recognition, we used Faster R-CNN algorithm in order to (i) detect the monitored object (*i.e.*, persons) and (ii) measure its surface to distinguish from the objects with a different surface. In addition to GUAVA, where only face recognition is performed, we consider GUAVA+ that combines both facial recognition and object surface measurement as illustrated in Figure 6.

Furthermore, using the monitored objects mobility patterns, we created an-

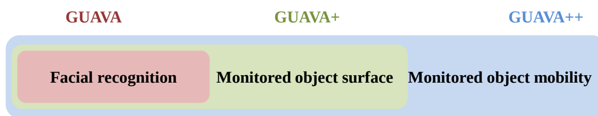

Figure 6: GUAVA different versions, with specific features.

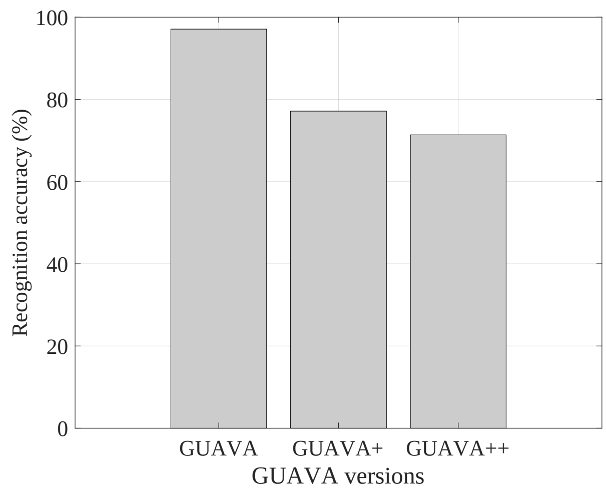

Figure 7: A recognition comparison between GUAVA different versions.

other version, namely GUAVA++, that besides facial recognition and object surface measurement, it filters out the potential duplication through the consideration of the mobility patterns of the monitored objects. This means that two objects with similar mobility patterns are considered as a same object. Obtained accuracy results are shown in Figure 7 and depict that adding these two features (*i.e.*, object surface measurement and mobility patterns) - surprisingly - results in a decrease of the overall accuracy. Indeed, since the surfaces of the people change with the movement of the arms and feets, the same person's surface is variable and hence considered as a different one. The mobility of persons can be effective only in sparse cases, not in high density scenarios. Hence, considering only the facial recognition can offer at least a 12% higher accuracy. Hence, considering only the facial recognition can offer at least a 12% higher accuracy.

4.2.2. Evaluation of QoS metrics

Figure 8 shows the packet delivery ratio when varying the UAVs/GVs density. It can be observed that the proposed scheme gives a significantly high PDR in the LTE environment. It is always above 99%, with a preference for UAVs but, as the density increases, it begins to gradually decrease due to the higher chances of packet collisions between simultaneous transmissions.

Other QoS metrics, such as the throughput and jitter, are depicted in Fig-

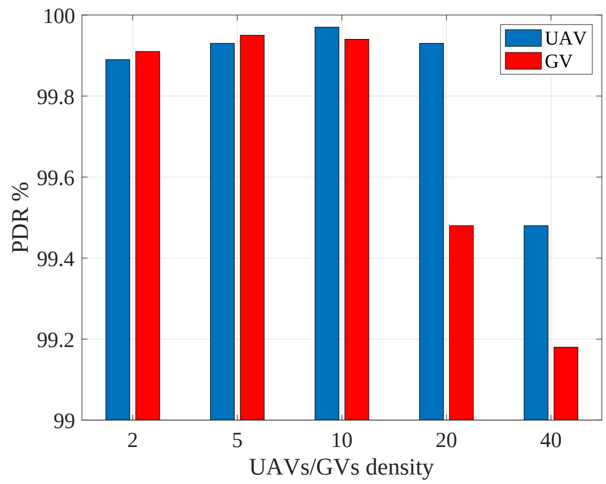

Figure 8: PDR variation vs. UAVs/GVs density.

ure 9 and Figure 13, respectively. As expected, Figure 9 describes how the average throughput Θ in the network increases with the UAVs/GVs density, thanks to the higher number of collected information. Similarly, in Figure 13 the mean jitter shows an increase while varying the vehicular density, due to higher collisions and congestion.

To show the benefits of the cooperation between GVs and UAVs, we compare GUAVA against a crowdsensing platform named BUCST [16], where the monitoring process is the task of UAVs only, while GVs act as communication backbone. As metrics, we study the traffic overhead and the convergence of both frameworks with respect to the monitored area and the required monitoring time.

It can be observed from Figure 10 that GUAVA introduces a reduced overhead compared to the BUCST monitoring overhead. This is due to (i) the cooperation of GVs and UAVs that act both as Collectors and (ii) the face recognition algorithm that avoids the transmission of duplicated data.

Figure 11 instead shows the time for monitoring an area taken by the BUCST and GUAVA, in a scenario consisting of 2 UAVs, 10 GV, and only 1 edge server (*i.e.*, Collection Center) in every 1 km^2. Obtained results shown that even with the considered minimal simulation settings, GUAVA is able to monitor up to 16 km^2 in about 10 minutes clearly bypassing the state-of-art work BUCST that reached less than 9 km^2 in a similar period of time. Again, this is mainly due to the efficient UAV-to-GV cooperation in GUAVA.

4.2.3. Energy consumption analysis

By introducing a separated energy model for the thermal cameras, we perform a simulation campaign to show how the UAVs batteries are affected with and without thermal cameras using the same mobility patterns [48]. Obtained

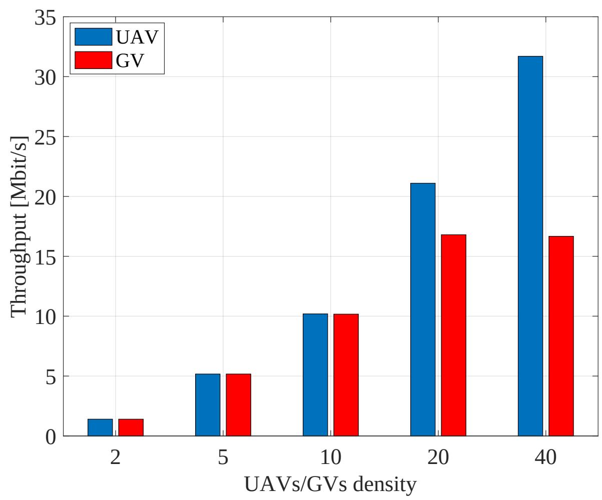

Figure 9: Throughput variation vs. UAVs/GVs density.

results depicted in Figure 12 show that the overall energy consumption is very slightly affected by the use of thermal cameras which is very acceptable compared to the additional value and applications brought by such devices.

To obtain further insight about the available lifetime of UAVs w.r.t. QoS guarantees, we can address the following optimization problem related to the minimization of the number of GVs and UAVs collectors (*i.e.*, $N_{GV/UAV}$) that can provide a minimum QoS level, expressed as (i) guaranteed minimum throughput Θ [Mb/s] and (ii) maximum achievable E2E delay d_{e2e} [ms] *i.e.*,

$$\begin{aligned} &\min N_{GV/UAV} \\ &s.t.\ \ \Theta \geq Th \\ &d_{e2e} \leq \delta \end{aligned} \tag{6}$$

where Th [Mb/s] represents the lower bound of achievable throughput threshold and δ [ms] is the upper bound of delay.

From Figure 4 and Figure 9, assuming different values of throughput Th and delay δ thresholds, we observe that the optimization problem defined in Eq. (6) provides the following solutions collected in Table 4. Notice that the minimum UAV/GV collector configuration comprised of $N = 10$ and $U = 10$ is achieved only for $Th = 10$ Mbit/s and $\delta = [20, 40, 60]$ ms. For increasing throughput thresholds, the number of UAVs increases while still guaranteeing the QoS requirements, but the minimum number of GVs is not achieved. Finally, in case of very high throughput requirement, neither UAVs or GVs can provide

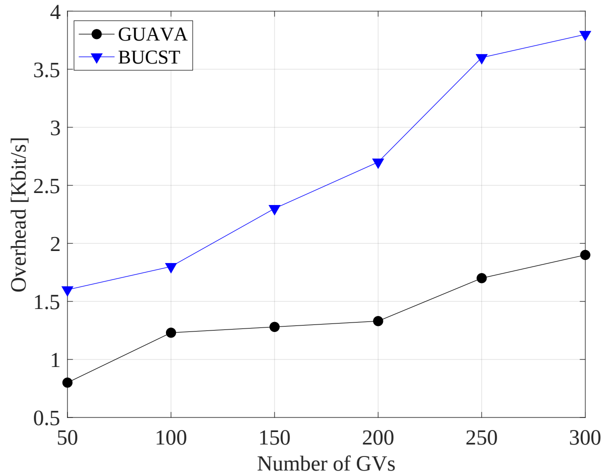

Figure 10: GUAVA additional overhead compared to BUCST.

the minimum configuration (*i.e.*, not available configuration).

5. Discussion and conclusion

5.1. Remarks

In this paper we presented a crowdsensing solution that takes advantage of both ground and flying vehicles to fight pandemic situations. The proposal, namely GUAVA, involves thermal camera based vital signs scanning and facial recognition to help identifying potentially infectious individuals and discarding duplicate sensed parameters. The performance assessment has consisted of two main parts *i.e.*, (*i*) the evaluation of the accuracy of the facial recognition algorithm, and (*ii*) the evaluation of the crowdsensing process in terms of network QoS metrics and overhead, which has been obtained through simulations with ns-3. Indeed, a first target of our analysis was to demonstrate the feasibility of the proposed approach in a realistic network scenario. Performance evaluation has shown that our design gives high performance in terms of various QoS metrics, as well as face recognition rates.

Compared to other existing models such as [9, 16, 17], our architecture enables the cooperation between UAVs and GVs, to detect and monitor the spread of Covid-19 in real time. It also provides the following benefits *i.e.*, (*i*) it ensures full coverage of city environments and hard-to-reach areas, (*ii*) it provides an energy efficient solution for the UAVs through wireless GV chargers, leveraging the GPS technology that provides location information of the nearest GV, (*iii*) it implements data offloading from UAVs to GVs, to deal with storage capacity and power consumption challenges, (*iv*) it leverages the LTE radio technology for data transmission, which gives the high performances in terms of QoS metrics, and (*v*) it can be exploited in various other applications, including fighting future pandemics and other disease like Ebola, tracking and identification of lost children or fugitives in crowded public places, such as streets, stadiums and

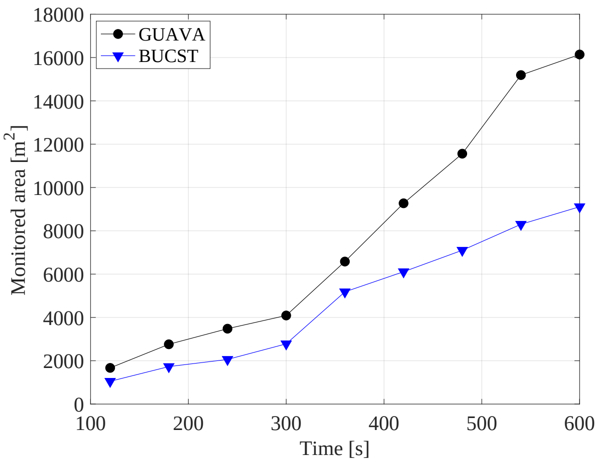

Figure 11: GUAVA area monitoring convergence compared to BUCST.

parks. The selected face recognition algorithm, namely GaussianFace, adopted in thermal cameras for real-time data duplication checks, outperforms most existing algorithms in terms of accuracy, with low training.

5.2. Implications for stakeholders

The proposed GUAVA framework involves three different groups of stakeholders with different roles and implications, *i.e.*, (*i*) Government authorities and agencies, (*ii*) citizens, and (*iii*) local authorities and health officials. The first category includes the Health Ministry and other permanent or semi-permanent state agencies that oversee, manage and issue at high level all the services related to the Covid-19 emergency. This implicates the need of ensuring privacy support to the citizens since GUAVA framework collects face images and body parameters of people in public areas, then exposing citizens to privacy risks. Although different countries have different societal norms and values, in principle Government Authorities and Agencies should ensure that collected data are not used for purposes beyond the pandemic. Moreover, they should guarantee that (*i*) the sensed data are not released to the public and (*ii*) they are treated and processed according to the existing privacy regulations. This aspect is very important also in case of false positive Covid-19 results: although the GUAVA framework is able to recognize people with Covid-19 symptoms, the final result about Covid-19 positivity should be always proved with a diagnostic test *e.g.* a molecular swab. Therefore, people recognized as potentially infectious should be quickly monitored with an additional test to prevent a false positive claim.

Also, it results necessary to estimate the economic impact of the adoption of GUAVA service, due to the set-up and management of the wireless crowdsensing devices with thermal cameras. Governments Authorities and Agencies have to perform a thorough feasibility study to identify the geographical areas

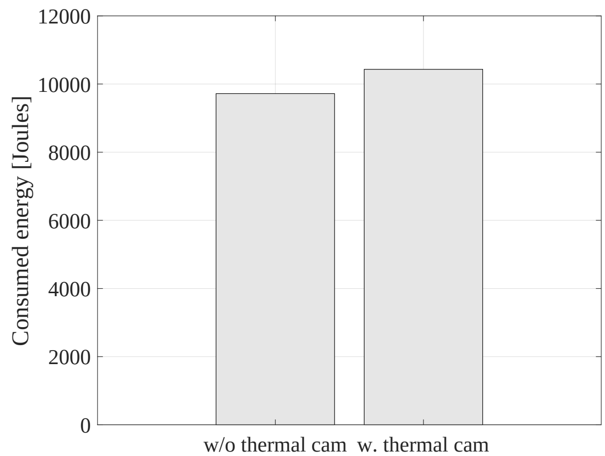

Figure 12: UAVs overall energy consumption at the end of the experiments both with and without thermal cameras.

where the GUAVA services are really required (*e.g.*, based on the reported daily cases, population density, etc.), thus balancing benefits and costs. To further maximize the benefits of investing in the GUAVA framework, other applications beyond the Covid-19 pandemic, *e.g.*, fugitive tracking, can be introduced in the framework. Finally, for local authorities and health officials, like the Police or specific public/private companies managing the GUAVA framework in practice, the usage of GUAVA implies the guarantee of people privacy, as well as the remote control of GV/UAV collectors.

5.3. Open Challenges

Although the conceived framework proved its effectiveness in the data collection process, there are still some open challenges in its practical deployment, as reported below:

- **Energy consumption of UAVs.** The recharging process of UAVs, which is needed from time to time, may lead to a temporary interruption of the crowdsensing service. To overcome this issue and guarantee a seamless service, an optimization strategy can be implemented. Based on the size of the geographic area to be covered and the approximately number of people to be detected and sensed, the duration of the UAV mission can be estimated. If this time exceeds the current battery lifetime of a single device, then the targeted geographic area can be divided into smaller regions that are assigned to more UAVs. Alternatively, a simpler approach would be to foresee the presence of a backup UAV that can complete the mission during the re-charging process of a previous UAV;

- **Smart selection of the targeted geographic areas.** Since the Collectors are wireless devices, the GUAVA crowdsensing process can be performed dynamically in different regions and according to the evolution of

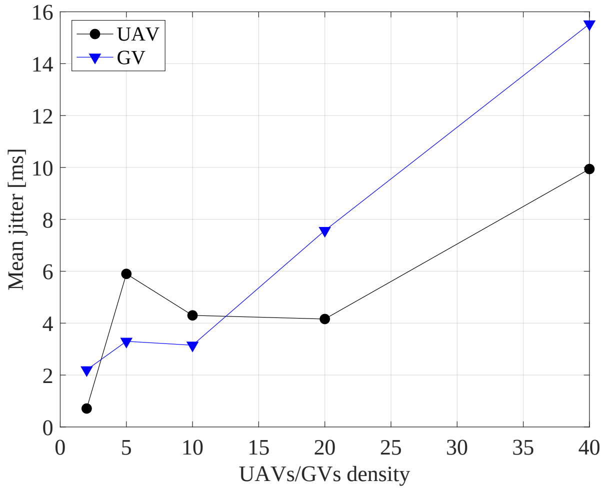

Figure 13: Mean jitter variation vs. UAVs/GVs density.

the epidemic. Of course, to maximize the benefits of GUAVA, its service cannot be executed indiscriminately but only in specific geographic areas, typically places of mass gathering or places were a high rate of infections is expected (*i.e.*, the so-called red zones). A non trivial preliminary task to be performed is therefore the identification of the areas to be sensed, together with other related information that can make the best of the UAVs usage, like the expected number of people to be sensed and the expected weather conditions;

- **Management of UAV flight operations.** As known, UAVs' missions are affected by weather conditions, especially strong winds, which may divert them from their path. Therefore, how to choose the optimum flight height to ensure full coverage in the designated area, without interference with other devices and obstacles, is not trivial, as well as if the UAV battery voltage drops down suddenly or a damage occurs, there is a crash risk and it is necessary to adopt security solutions, such as using small parachutes;

- **Twins detection.** Concerning the face recognition process, we observe that the possible presence of look-alike faces, like twins, can make the process more challenging and additional techniques are needed to cope against such similarity issues. Moreover, with the advancements of face recognition technology, Deepfakes techniques that deceive existing algorithms [49] can also spread. It is therefore necessary to use a hybrid system that does not rely on a facial recognition technique only, but also associates it with other recognition modalities, such as upper-body recognition [50] (*e.g.*, shoulder-to-shoulder width, neck length/width, chest/waist size and back length, etc.). Fusing the two recognition modalities would allow us to improve the accuracy of the overall recognition process.

Our future work will be devoted to solving the above mentioned open issues. In particular, after proving the feasibility of the GUAVA framework, the next evaluation step will be the creation of a prototype including a small set of Collectors, *e.g.*, a GV acting as collector and re-charging station and a couple of UAVs. The prototype will be also devoted to better study and improve the accuracy of the face recognition process in presence of look-alike people like twins. This can be done by combining other existing biometric technologies with facial recognition, such as gait biometrics, in order to address the similarity issue in people's faces.

Acknowledgment

This work was supported by the Deanship of Scientific Research at Prince Sattam bin Abdulaziz University, Saudi Arabia.

References

[1] H. Ma, D. Zhao, P. Yuan, Opportunities in mobile crowd sensing, IEEE Communications Magazine 52 (8) (2014) 29–35.

[2] J. M. Cecilia, J.-C. Cano, E. Hernández-Orallo, C. T. Calafate, P. Manzoni, Mobile crowdsensing approaches to address the covid-19 pandemic in spain, IET Smart Cities 2 (2) (2020) 58–63.

[3] E. Hernández-Orallo, C. T. Calafate, J.-C. Cano, P. Manzoni, Evaluating the effectiveness of covid-19 bluetooth-based smartphone contact tracing applications, Applied Sciences 10 (20) (2020) 7113.

[4] G. Quer, J. M. Radin, M. Gadaleta, K. Baca-Motes, L. Ariniello, E. Ramos, V. Kheterpal, E. J. Topol, S. R. Steinhubl, Wearable sensor data and self-reported symptoms for covid-19 detection, Nature Medicine (2020) 1–5.

[5] X.-R. Ding, D. Clifton, J. Nan, N. H. Lovell, P. Bonato, W. Chen, X. Yu, Z. Xue, T. Xiang, X. Long, et al., Wearable sensing and telehealth technology with potential applications in the coronavirus pandemic, IEEE Reviews in Biomedical Engineering (2020).

[6] Y. Sahraoui, A. Korichi, C. A. Kerrache, M. Bilal, M. Amadeo, Remote sensing to control respiratory viral diseases outbreaks using internet of vehicles, Transactions on Emerging Telecommunications Technologies (2020) e4118.

[7] X. Zhu, Y. Luo, A. Liu, W. Tang, M. Z. A. Bhuiyan, A deep learning-based mobile crowdsensing scheme by predicting vehicle mobility, IEEE Transactions on Intelligent Transportation Systems (2020).

[8] B. Wang, Y. Sun, D. Liu, H. M. Nguyen, T. Q. Duong, Social-aware uav-assisted mobile crowd sensing in stochastic and dynamic environments for disaster relief networks, IEEE Transactions on Vehicular Technology 69 (1) (2019) 1070–1074.

[9] A. Kumar, K. Sharma, H. Singh, S. G. Naugriya, S. S. Gill, R. Buyya, A drone-based networked system and methods for combating coronavirus disease (covid-19) pandemic, Future Generation Computer Systems 115 (2020) 1–19.

[10] J. Liu, H. Shen, H. S. Narman, W. Chung, Z. Lin, A survey of mobile crowdsensing techniques: A critical component for the internet of things, ACM Transactions on Cyber-Physical Systems 2 (3) (2018) 1–26.

[11] C. Wang, C. Li, C. Qin, W. Wang, X. Li, Maximizing spatial–temporal coverage in mobile crowd-sensing based on public transports with predictable trajectory, International Journal of Distributed Sensor Networks 14 (8) (2018) 1550147718795351.

[12] Z. Xu, W. Yang, Z. Xiong, J. Wang, G. Liu, Tpsense: A framework for event-reports trustworthiness evaluation in privacy-preserving vehicular crowdsensing systems, Journal of Signal Processing Systems (2020) 1–11.

[13] L. Shao, C. Wang, L. Liu, C. Jiang, Rts: road topology-based scheme for traffic condition estimation via vehicular crowdsensing, Concurrency and Computation: Practice and Experience 29 (3) (2017) e3778.

[14] A. M. Elbir, G. Gurbilek, B. Soner, S. Coleri, Vehicular networks for combating a worldwide pandemic: Preventing the spread of covid-19, arXiv preprint arXiv:2010.07602 (2020).

[15] Y. Sahraoui, C. A. Kerrache, A. Korichi, B. Nour, A. Adnane, R. Hussain, Deepdist: A deep-learning-based iov framework for real-time objects and distance violation detection, IEEE Internet of Things Magazine 3 (3) (2020) 30–34.

[16] E. Barka, C. A. Kerrache, N. Lagraa, A. Lakas, Behavior-aware uav-assisted crowd sensing technique for urban vehicular environments, in: 2018 15th IEEE Annual Consumer Communications & Networking Conference (CCNC), IEEE, 2018, pp. 1–7.

[17] A. Trotta, U. Muncuk, M. Di Felice, K. R. Chowdhury, Persistent crowd tracking using unmanned aerial vehicle swarms: A novel framework for energy and mobility management, IEEE Vehicular Technology Magazine 15 (2) (2020) 96–103.

[18] N. H. Motlagh, M. Bagaa, T. Taleb, Uav-based iot platform: A crowd surveillance use case, IEEE Communications Magazine 55 (2) (2017) 128–134.

[19] M. Zhang, X. Li, Drone-enabled internet of things relay for environmental monitoring in remote areas without public networks, IEEE Internet of Things Journal (2020).

[20] R. Vera-Amaro, M. E. Rivero-Ángeles, A. Luviano-Juárez, Data collection schemes for animal monitoring using wsns-assisted by uavs: Wsns-oriented or uav-oriented, Sensors 20 (1) (2020) 262.

[21] C. Luo, J. Nightingale, E. Asemota, C. Grecos, A uav-cloud system for disaster sensing applications, in: 2015 IEEE 81st Vehicular Technology Conference (VTC Spring), IEEE, 2015, pp. 1–5.

[22] Y. Siriwardhana, G. Gür, M. Ylianttila, M. Liyanage, The role of 5g for digital healthcare against covid-19 pandemic: Opportunities and challenges, ICT Express (2020).

[23] V. Chamola, V. Hassija, V. Gupta, M. Guizani, A comprehensive review of the covid-19 pandemic and the role of iot, drones, ai, blockchain, and 5g in managing its impact, IEEE Access 8 (2020) 90225–90265.

[24] F.-T.-Z. Khanam, L. A. Chahl, J. S. Chahl, A. Al-Naji, A. G. Perera, D. Wang, Y. Lee, T. T. Ogunwa, S. Teague, T. X. B. Nguyen, et al., Noncontact sensing of contagion, Journal of Imaging 7 (2) (2021) 28.

[25] K. Yi, R. Du, L. Liu, Q. Chen, K. Gao, Fast participant recruitment algorithm for large-scale vehicle-based mobile crowd sensing, Pervasive and Mobile Computing 38 (2017) 188–199.

[26] S. Kluge, U. Janssens, T. Welte, S. Weber-Carstens, G. Marx, C. Karagiannidis, German recommendations for critically ill patients with covid-19, Medizinische Klinik, Intensivmedizin und Notfallmedizin (2020) 1.

[27] G. Sun, Y. Nakayama, S. Dagdanpurev, S. Abe, H. Nishimura, T. Kirimoto, T. Matsui, Remote sensing of multiple vital signs using a cmos camera-equipped infrared thermography system and its clinical application in rapidly screening patients with suspected infectious diseases, International Journal of Infectious Diseases 55 (2017) 113–117.

[28] G. Sun, T. Negishi, T. Kirimoto, T. Matsui, S. Abe, Noncontact monitoring of vital signs with rgb and infrared camera and its application to screening of potential infection, in: Non-Invasive Diagnostic Methods-Image Processing, IntechOpen, 2018.

[29] C. Lu, X. Tang, Surpassing human-level face verification performance on lfw with gaussianface, in: Proceedings of the AAAI Conference on Artificial Intelligence, Vol. 29, 2015.

[30] S. Morton, R. D'Sa, N. Papanikolopoulos, Solar powered uav: Design and experiments, in: IEEE/RSJ International Conference on Intelligent Robots and Systems (IROS), 2015, pp. 2460–2466.

[31] S. Jung, Y. Jo, Y.-J. Kim, Flight time estimation for continuous surveillance missions using a multirotor uav, Energies 12 (5) (2019) 867.

[32] K. Rawat, E. Lawrence, A mini-uav vtol platform for surveying applications, IAES International Journal of Robotics and Automation 3 (4) (2014) 259.

[33] G. Rossi, L. Tanteri, V. Tofani, P. Vannocci, S. Moretti, N. Casagli, Multitemporal uav surveys for landslide mapping and characterization, Landslides 15 (5) (2018) 1045–1052.

[34] 3GPP, TS 23.285 v15.2.0. Technical Specification Group Services and System Aspects; Architecture enhancements for V2X services, release 15 (December 2018).

[35] T. Bourlai, B. Cukic, Multi-spectral face recognition: Identification of people in difficult environments, in: 2012 IEEE International Conference on Intelligence and Security Informatics, IEEE, 2012, pp. 196–201.

[36] T. Bourlai, J. Von Dollen, N. Mavridis, C. Kolanko, Evaluating the efficiency of a night-time, middle-range infrared sensor for applications in human detection and recognition, in: Infrared Imaging Systems: Design, Analysis, Modeling, and Testing XXIII, Vol. 8355, International Society for Optics and Photonics, 2012, p. 83551B.

[37] D. A. Berlin, R. M. Gulick, F. J. Martinez, Severe covid-19, New England Journal of Medicine (2020).

[38] X. Wang, J. Fang, Y. Zhu, L. Chen, F. Ding, R. Zhou, L. Ge, F. Wang, Q. Chen, Y. Zhang, et al., Clinical characteristics of non-critically ill patients with novel coronavirus infection (covid-19) in a fangcang hospital, Clinical Microbiology and Infection (2020).

[39] Q. Ke, J. Liu, M. Bennamoun, S. An, F. Sohel, F. Boussaid, Computer vision for human–machine interaction, in: Computer Vision for Assistive Healthcare, Elsevier, 2018, pp. 127–145.

[40] M. M. Ghazi, H. K. Ekenel, A comprehensive analysis of deep learning based representation for face recognition, arXiv preprint arXiv:1606.02894 (2016).

[41] G. B. Huang, M. Ramesh, T. Berg, E. Learned-Miller, Labeled faces in the wild: A database for studying face recognition in unconstrained environments.

[42] R. Urtasun, T. Darrell, Discriminative gaussian process latent variable model for classification, in: Proceedings of the 24th international conference on Machine learning, 2007, pp. 927–934.

[43] SUMO (Simulation of Urban MObility), http://sumo.sourceforge.net (accessed October 2, 2020).

[44] D. Broyles, A. Jabbar, J. P. Sterbenz, et al., Design and analysis of a 3–d gauss-markov mobility model for highly-dynamic airborne networks, in: Proceedings of the international telemetering conference (ITC), San Diego, CA, 2010, pp. 25–28.

[45] Y. Sahraoui, A. Korichi, C. A. Kerrache, M. Bilal, M. Amadeo, Remote sensing to control respiratory viral diseases outbreaks using internet of vehicles, Emerging Telecommunications Technologies (2020).

[46] P. J. Phillips, H. Wechsler, J. Huang, P. J. Rauss, The feret database and evaluation procedure for face-recognition algorithms, Image and vision computing 16 (5) (1998) 295–306.

[47] Y.-Q. Wang, An analysis of the viola-jones face detection algorithm, Image Processing On Line 4 (2014) 128–148.

[48] S. Akbari, Studying window energy performance using thermal camera, Ph.D. thesis, North Dakota State University (2020).

[49] P. Korshunov, S. Marcel, Deepfakes: a new threat to face recognition? assessment and detection, arXiv preprint arXiv:1812.08685 (2018).

[50] K. Kim, Z. Yang, I. Masi, R. Nevatia, G. Medioni, Face and body association for video-based face recognition, in: 2018 IEEE Winter Conference on Applications of Computer Vision (WACV), IEEE, 2018, pp. 39–48.

Algorithm 1: Pseudocode of the GUAVA crowdsensing process for UAVs

Input :
$G = \{g_1, g_2, \ldots, g_i, \ldots, g_N\}$ with $i \leq N$ and $N \in \mathbb{N}$ ▷ Set of GVs
$U = \{u_1, u_2, \ldots, u_j, \ldots, u_M\}$ with $j \leq M$ and $M \in \mathbb{N}$ ▷ Set of UAVs
$P = \{p_1, p_2, \ldots, p_k, \ldots, p_K\}$ with $k \leq K$ and $K \in \mathbb{N}$ ▷ Set of people
$\mathcal{I}_s$ ▷ Set of stored images
$\mathcal{E}_{u_j}$ ▷ Battery level of UAV u_j
χ ▷ Warning threshold for batter level
Output: $\mathcal{I}_s$ ▷ Updated set of suspected cases
if $\mathcal{E}_{u_j} > \chi$ **then**
  while $\|\overrightarrow{l_{u_j}} - \overrightarrow{l_{p_k}}\| \leq r_s^{(j)}$ **do**
    $\overrightarrow{V}_{s1,k},\ \overrightarrow{V}_{s2,k}$ ▷ Sensing vital signs from the thermal video
    Γ ▷ Extract faces from thermal video
    foreach $\Gamma \notin \mathcal{I}_s$ **do**
      $\mathcal{I}_s \leftarrow \mathcal{I}_s \cup \Gamma$
      if $\overrightarrow{V}_{s1,k} \geq \tau_1$ AND $\overrightarrow{V}_{s2,k} \geq \tau_2$ **then**
        Send the information to the edge server ▷ Possible p_k infected
      else
        Discard this case
else
  $\min_i d_{u_j,g_i},\ \ \forall g_i \in G$ ▷ Compute the distance to the closest GV
  Move to position $\overrightarrow{l_{g_i}}$ ▷ Wireless charging from the closest GV
  Offloading $\mathcal{I}_s$ to g_i
while $\|\overrightarrow{l_{g_i}} - \overrightarrow{l_{p_k}}\| \leq r_s^{(i)}$ **do**
  $\overrightarrow{V}_{s1,k},\ \overrightarrow{V}_{s2,k}$ ▷ Sensing vital signs from the thermal video
  Γ ▷ Extract faces from thermal video
  foreach $\Gamma \notin \mathcal{I}_s$ **do**
    $\mathcal{I}_s \leftarrow \mathcal{I}_s \cup \Gamma$
    if $\overrightarrow{V}_{s1,k} \geq \tau_1$ AND $\overrightarrow{V}_{s2,k} \geq \tau_2$ **then**
      Send the information to the edge server ▷ Possible p_k infected
    else
      Discard this case

Table 2: Simulation parameters.

	Simulation parameters	**Values**
General	Communication technology	LTE + wired
	Simulation Time	50 seconds
	UAVs density	2, 5, 10, 20, 40 [UAV/km^2]
	Number of eNB	1
	UAVs' mobility model	Gauss Markov 3D
	Simulation flight area	200×200 m
	Speed of UAVs (velocity)	20 m/s
	UAVs flight height	30 m
	Data packet size	1024
LTE	GVs propagation loss model	Nakagami
	UAVs propagation loss model	Friis
	LTE data packet type	TCP
	Transmission power	eNB (49 dBm)/UE (23 dBm)
	GVs density	2, 5, 10, 20, 40 [UAV/m^2]
	Simulation ground area	1471.47×1989.8 [m^2]

Table 3: Error rate result.

Probe dataset size	Probe images	Error rate
623 images	 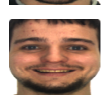 Facial expressions	3.69%

Table 4: Configuration pairs of minimum UAVs (*i.e.*, N) and GVs (*i.e.*, U) collectors achieving different throughput Th (*i.e.*, $Th = [10, 20, 30]$ Mbit/s) and E2E delay (*i.e.*, $\delta = [20, 40, 60]$ ms) thresholds.

		E2E delay threshold		
		20	40	60
Throughput threshold	10	$(N = 10, U = 10)$	$(N = 10, U = 10)$	$(N = 10, U = 10)$
	20	$(N = 0, U = 20)$	$(N = 0, U = 20)$	$(N = 0, U = 20)$
	30	n/a	n/a	$(N = 0, U = 40)$